

This work was written as part of one of the author's official duties as an Employee of the United States Government and is therefore a work of the United States Government. In accordance with 17 U.S.C. 105, no copyright protection is available for such works under U.S. Law. Access to this work was provided by the University of Maryland, Baltimore County (UMBC) ScholarWorks@UMBC digital repository on the Maryland Shared Open Access (MD-SOAR) platform.

Please provide feedback

Please support the ScholarWorks@UMBC repository by emailing scholarworks-group@umbc.edu and telling us what having access to this work means to you and why it's important to you. Thank you.

Transit time of chirped pulses through one-dimensional, nonabsorbing barriers

G. D'Aguanno and M. Centini

*Dipartimento di Energetica, Istituto Nazionale per la Fisica della Materia,
Università di Roma "La Sapienza," Via A. Scarpa 16, I-00161 Rome, Italy and
Weapons Sciences Directorate, Research Development and Engineering Center, U.S. Army Aviation and Missile Command,
Building 7804, Redstone Arsenal, Alabama 35898-5000*

M. J. Bloemer, K. Myneni, M. Scalora, and C. M. Bowden

*Weapons Sciences Directorate, Research Development and Engineering Center, U.S. Army Aviation and Missile Command,
Building 7804, Redstone Arsenal, Alabama 35898-5000*

C. Sibilio and M. Bertolotti

*Istituto Nazionale per la Fisica della Materia, Dipartimento di Energetica, Università di Roma "La Sapienza,"
Via A. Scarpa 16, I-00161 Rome, Italy*

Received October 2, 2001

Experiments show that the transit times of chirped, narrow-band pulses that move across nonabsorbing, one-dimensional barriers are modified dramatically by the interplay between the chirp and the transmission function of the sample. In an experiment we monitored 0.9-ns chirped, nearly Gaussian pulses as they traversed a 450- μm GaAs etalon. At certain wavelengths pulse transit times can be superluminal or even negative. To explain these phenomena we have proposed a generalization of the transit time for chirped pulses that is still meaningful even when the transit times are superluminal or negative. Our predictions agree well with the experimental results. © 2002 Optical Society of America

OCIS codes: 240.0310, 230.4170, 190.5530.

The transit time of optical pulses traversing different types of media has been a topic of interest for many years.¹⁻³ For an incident pulse whose spectral bandwidth is sharply peaked about a specific value ω_0 of transmittance spectrum $T(\omega)$ of a one-dimensional, nonabsorbing optical barrier, the time that the transmitted part of the pulse takes to traverse the structure is the phase time⁴ (or group delay), defined as $\tau(\omega_0) \equiv (d\phi_t(\omega)/d\omega)|_{\omega=\omega_0}$, where $\phi_t(\omega)$ is the phase of the transmission function, $t_\omega = \sqrt{T(\omega)} \exp[i\phi_t(\omega)]$. So we ask: What happens if the input pulse is chirped, such that it remains sharply peaked about the same frequency ω_0 of the transmission spectrum? Under these circumstances, can the phase time accurately predict the transit time? Is it still meaningful to consider a transit time, or must we abandon the concept of transit time because pulse distortion is so extreme as to render the concept unclear?

To answer these questions we performed a simple experiment in which we measured transit time as a function of wavelength for an optical pulse transiting a 450- μm GaAs substrate polished at both ends. The surfaces were not antireflection coated, so there were residual reflections, which resulted in etalon effects. In our experiment, the laser diode (New Focus, Inc., Model 6328 tunable laser) produces approximately Gaussian pulses (in the central region) of the type $A_0(t) = A_0 \exp[-(t^2/2\tau_0^2) - i\gamma t^2]$, where $\tau_0 = \tau_{\text{FWHM}}/(2\sqrt{\ln 2})$, $\tau_{\text{FWHM}} \approx 0.9$ ns, and $\gamma \approx -7 \times 10^{18} \text{ s}^{-2}$ is the magnitude of the chirp. The

sample was positioned between the laser head and a high-speed detector (New Focus Model 1611 InGaAs detector with a 1-GHz bandwidth). The detector output was observed on an HP 54750A digitizing oscilloscope with an HP 54751A, 20-GHz module. We determined the peak position to an uncertainty of 1–2 ps by fitting the waveform data about the peak region with a third-order polynomial. The total path without the sample served as the baseline. The sample was then inserted into the optical path, and the time difference (the delay time) recorded. The transit time was then obtained by addition of the free-space propagation time to the delay time. The results of the experiment are given in Fig. 1, where we also show the measured transmittance of the sample and the spectral bandwidth of a typical input pulse. In the figure, the transit times predicted from the phase times and the measured transit times have discrepancies that are well in excess of 100%. Agreement between the two times persists only at the peaks and valleys of the transmission function. We also found cases that correspond to negative transit times, in which the peak of the transmitted pulse appears on the other side of the barrier before the peak of the incident pulse enters the barrier.

The skeptical reader might think that in our experiment the transmitted part of the pulse is so drastically reshaped that the concept of transit time becomes vague. Indeed, such is not the case. Pulses do undergo small distortion, only in the wing regions, but

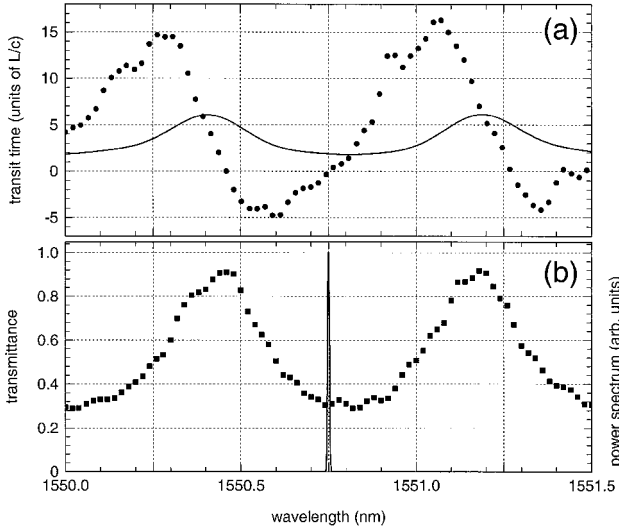


Fig. 1. (a) Measured transit time (dotted curve) and predicted phase time (solid curve) versus wavelength ($\lambda_0 = 2\pi c/\omega_0$) in units of L/c ($= 1.5$ ps) for a 0.9-nm Gaussian pulse propagating through an $L = 450$ μm GaAs Fabry–Perot etalon (ω_0 is the carrier frequency). The chirp coefficient is $\gamma \approx -7 \times 10^{18} \text{ s}^{-2}$. (b) Measured transmittance of the sample (filled squares) and Fourier spectrum of a typical incident chirped pulse (continuous curve). The pulse is sharply peaked with respect to the transmission function and is approximately 40 times smaller than the FWHM of resonance bandwidth.

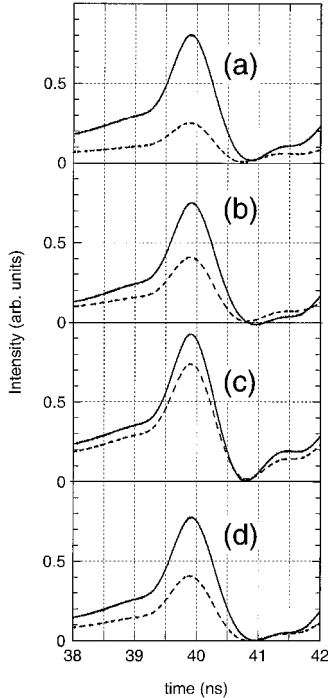


Fig. 2. Four snapshots of the incident (solid curves) and the transmitted (dashed curves) pulses that have the following carrier wavelengths (b): (a) 1550.8 nm, (transmission minimum), (b) 1551 nm, (c) 1551.2 nm (transmission maximum), (d) 1551.3 nm.

from Fig. 2 one can clearly still determine the location of the peak of the pulse and monitor it to extract the transit time. Below, we shall see that it is possible to

generalize the notion of phase time to still accurately predict the transit time.

We begin with the wave equation $\partial^2 f / \partial z^2 - [n^2(z)/c^2] \partial^2 f / \partial t^2 = 0$, such that $n(z) = 1$ for $z > L$ and $z < 0$, and $n(z) = n_0$ for $0 \leq z \leq L$ ($n_0 \approx 3.37$ for GaAs in the wavelength range of interest), so $n(z)$ is real. The solution of the wave equation at $z = L$ for the transmitted field is $f(L, t) = (1/2\pi) \int_{-\infty}^{+\infty} \tilde{f}(L, \omega) \exp(-i\omega t) d\omega$, where

$$\begin{aligned} \tilde{f}(L, \omega) &= \sqrt{T(\omega)} \exp[i\phi_t(\omega)] \tilde{f}(0, \omega) \\ &= \exp(i\{\phi_t(\omega) - (i/2)\ln[T(\omega)]\}) \tilde{f}(0, \omega) \end{aligned}$$

and $\tilde{f}(0, \omega) = \text{FT}\{f(0, t)\}$. FT is the Fourier-transform operator. For convenience we may define an effective, complex wave vector $\hat{k}(\omega) = \hat{n}(\omega)\omega/c$; $\hat{n}(\omega) = (c/L\omega)\{\phi_t(\omega) - (i/2)\ln[T(\omega)]\}$ is the effective index of the barrier that satisfies that Kramers–Kronig relations.⁵ Then the solution of the wave equation for the transmitted field, without approximations, takes the following form: $f(L, t) = (1/2\pi) \int_{-\infty}^{+\infty} \tilde{f}(0, \omega) \exp\{i[\hat{k}(\omega)L - \omega t]\} d\omega$. We consider a linearly chirped, Gaussian pulse with carrier frequency ω_0 such that, at $z = 0$, $f(0, t) = A_0(t) \exp(-i\omega_0 t)$ and $A_0(t) = A_0 \exp[-(t^2/2\tau_0^2) - i\gamma t^2]$. So at $t = 0$ the peak of the pulse is located at $z = 0$. For the transmitted field we obtain $f(L, t) = (1/2\pi) \int_{-\infty}^{+\infty} \tilde{A}_0(\omega - \omega_0) \exp\{i[\hat{k}(\omega)L - \omega t]\} d\omega$, where $\tilde{A}_0(\omega) = \text{FT}\{A_0(t)\}$. We expand the propagator about carrier frequency ω_0 up to first order⁶ and obtain

$$\begin{aligned} \hat{k}(\omega) &\cong \frac{1}{L} \left(\{\phi_t(\omega_0) - (i/2)\ln[T(\omega_0)]\} \right. \\ &\quad \left. + \left[\tau(\omega_0) - i \frac{\delta}{2} \right] (\omega - \omega_0) \right), \end{aligned} \quad (1)$$

where $\delta = [dT(\omega)/d\omega]_{\omega=\omega_0}/T(\omega_0)$ is a parameter that depends on the transmission of the structure, and $\tau(\omega_0) \equiv [d\phi_t(\omega)/d\omega]_{\omega=\omega_0}$ is the phase time calculated at the carrier frequency.

After substituting expression (1) into the expression for the transmitted field, $f(L, t)$, and performing the resulting integral, we arrive at the expression for the transmitted field intensity:

$$\begin{aligned} |f(L, t)|^2 &= A_0^2 T(\omega_0) \exp\left(\frac{\delta^2}{4\tau_0^2} + \delta^2 \gamma^2 \tau_0^2\right) \\ &\quad \times \exp\left(-\frac{\{t - [\tau(\omega_0) + \delta \gamma \tau_0^2]\}^2}{\tau_0^2}\right). \end{aligned} \quad (2)$$

Equation (2) suggests that, whereas the amplitude of the transmitted pulse is rescaled, the output pulse remains Gaussian in shape. From Eq. (2), one may also extract the time t_{transit} that the peak of the pulse takes to propagate from ($z = 0, t = 0$) to $z = L$ because it is the time for which Eq. (2) is maximized. We find that

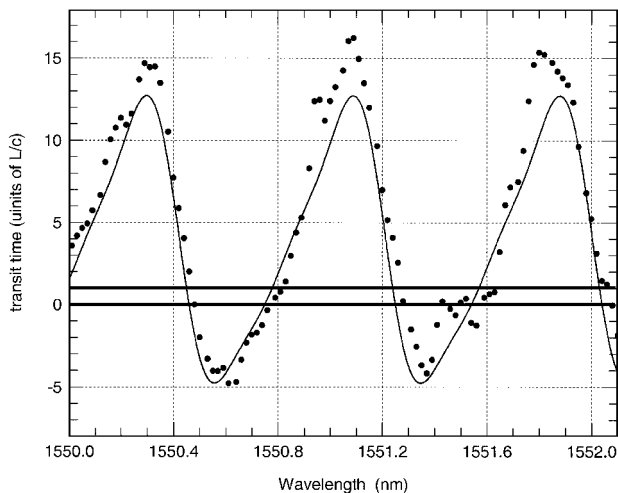


Fig. 3. Measured transit time (filled circles) and predicted transit time [solid curve, i.e., $t_{\text{transit}} = \tau(\omega_0) + \delta\gamma\tau_0^2$] for the structure of Fig. 1. The horizontal thick solid lines delimit superluminal transit times. Transit times are subluminal when $t_{\text{transit}} \geq L/c$ and are negative when $t_{\text{transit}} \leq 0$.

$$t_{\text{transit}} = \tau(\omega_0) + \delta\gamma\tau_0^2. \quad (3)$$

In Fig. 3 we compare the experimentally measured transit times and the transit times predicted by Eq. (3). The agreement between the two curves is evident, and Eq. (3) clearly represents an accurate generalization of the more-traditional phase time.

In Fig. 4 we compare the transmitted field obtained by using Eq. (2) with the transmitted field that we obtained by numerically integrating the wave equation. We also depict the pulse after it has propagated a distance of $450 \mu\text{m}$ in free space. The envelope of the transmitted pulse is contained well within the envelope of the freely propagating pulse.

In conclusion, we have discussed the properties of narrow-band chirped pulses that traverse nonabsorbing structures of finite length. We have provided theoretical and experimental evidence that the structure is only partly responsible for the delay imparted to the incident pulse; the total delay also depends on the exact nature of the incident pulse itself, a fact that to our knowledge is usually overlooked.

We thank J. W. Haus and B. Wendling for interesting discussions. G. D'Aguanno and M. Centini thank the U.S. Army European Research Office for partial financial support (grant R&D 8766-PH-01). M. Scalora's e-mail address is mscalora@ws.redstone.army.mil. G. D'Aguanno's e-mail address is giuseppe.daguanno@uniroma1.it.

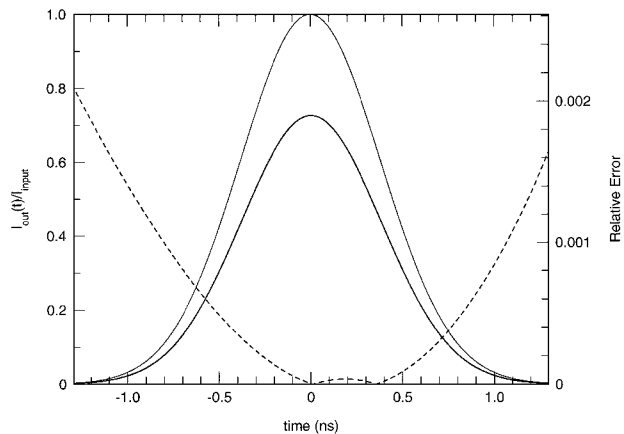


Fig. 4. Comparison of the numerical and the analytical solutions for the intensity of an output pulse that corresponds to an input chirped, 0.9-ns Gaussian pulse propagating through an $L = 450 \mu\text{m}$ GaAs Fabry–Perot etalon. The intensity of the output pulses (thicker solid curve) is normalized with respect to the peak intensity of the input pulse. The two curves are indistinguishable at this scale. The carrier wavelength of the pulse is $\sim 1550.55 \text{ nm}$, corresponding to a transmittance of $\sim 70\%$ and a negative transit time (Fig. 1). The relative error (dashed curve) between Eq. (2) and the solution of the wave equation, as outlined in the text, is defined as $|[I_{\text{out}}^{\text{numerical}}(t) - I_{\text{out}}^{\text{analytical}}(t)]/I_{\text{out}}^{\text{numerical}}(t)|$. Note that the relative error is less than 1 part in 10^5 in the central region of the pulse. The thinner solid curve depicts the same input pulse after it has propagated a distance of $450 \mu\text{m}$ in free space.

References

1. A. Dogariu, A. Kuzmich, and L. J. Wang, *Phys. Rev. A* **63**, 053806(1-11) (2001), and extended references therein.
2. A. Dogariu, A. Kuzmich, L. J. Wang, P. W. Milonni, and R. Y. Chiao, *Phys. Rev. Lett.* **86**, 3925 (2001).
3. G. D'Aguanno, M. Centini, M. Scalora, C. Sibilia, M. J. Bloemer, C. M. Bowden, J. W. Haus, and M. Bertolotti, *Phys. Rev. E* **63**, 036610(1-5) (2001).
4. For definitions of the various tunneling times the reader may consult R. T. Chiao and A. M. Steinberg, in *Progress in Optics*, E. Wolf, ed. (Elsevier, North Holland, Amsterdam, 1997), Vol. XXXVII, p. 345, and references therein.
5. M. Centini, C. Sibilia, M. Scalora, G. D'Aguanno, M. Bertolotti, M. J. Bloemer, C. M. Bowden, and I. Nefedov, *Phys. Rev. E* **60**, 4891 (1999).
6. The first-order expansion is justified because the spectral bandwidth of the pulse remains sharply peaked at all times with respect to transmission spectrum $T(\omega)$ [Fig. 1(b)].